Infrared Spectra of $M(OH)_{1,2,4}$ (M = Pb, Sn) in Solid Argon

Xuefeng Wang and Lester Andrews*

Chemistry Department, University of Virginia, Charlottesville, Virginia 22904-4319

Received: June 23, 2005; In Final Form: August 10, 2005

Infrared absorptions for the matrix-isolated lead and tin hydroxides M(OH), $M(OH)_2$ and $M(OH)_4$ (M = Pb, Sn) were observed in laser-ablated metal atom reactions with H_2O_2 during condensation in excess argon. The major $M(OH)_2$ product was also observed with H_2 and O_2 mixtures, which allowed the substitution of $^{18}O_2$. The band assignments were confirmed by appropriate D_2O_2, D_2, $^{16}O^{18}O$, and $^{18}O_2$ isotopic shifts. MP2 and B3LYP calculations were performed to obtain molecular structures and to reproduce the infrared spectra. The minimum energy structure found for $M(OH)_2$ has C_s symmetry and a weak intramolecular hydrogen bond. In experiments with Sn, HD, and O_2, the internal D bond is favored over the H bond for Sn(OH)(OD). The $Pb(OH)_4$ and $Sn(OH)_4$ molecules are calculated to have S_4 symmetry and substantial covalent character.

Introduction

Lead is one of the most common dispersed heavy metals in the atmosphere in the modern industrial era.[1−3] The toxicity on living organisms has been confirmed as displacement of vital metals in the organism leading to anemia and damage to the nervous system.[4,5] The PbOH radical might be produced in the atmosphere, but no definitive experimental observation has been made based on our knowledge.[6] However, two weak, broad near-infrared emission bands in a study of lead monohalides have been tentatively assigned to HPbO (or PbOH).[7]

The reactions of lead and tin with H_2 and O_2 in solid matrices have been studied separately, and the MO, MO_2, MH_2, and MH_4 molecules have been identified through infrared spectra.[8,9] The analogous SnX_2, SnX_4, and PbX_2 (X = Cl, Br, I) molecules have been observed by electron diffraction.[10] However, tetravalent lead is not stable since relativistic effects reduce the M−X bond strength, so only $PbCl_4$ has been observed experimentally.[10,11] It is very interesting to consider the lead and tin hydroxide molecules and their bonding and structure since very little is known about group 14 metal hydroxides.[12a] Solubility product constant data indicate that $Sn(OH)_2$ and $Pb(OH)_2$ are very weak bases, much weaker than $Mg(OH)_2$.[12b]

Recently we developed a new method to investigate metal hydroxide molecules using laser-ablated metal atom reactions with H_2O_2 or $H_2 + O_2$ mixtures in low-temperature matrices.[13] With this approach we have the advantage to identify most infrared active modes without overlapping excess water absorptions. For example, ionic $M(OH)_2$ (M = group 2 metals), ionic $M(OH)_2$ and $M(OH)_4$ (M = group 4 metals), and covalent $M(OH)_2$ molecules (M = group 12 metals) have been investigated. We present here a matrix infrared spectroscopic study of laser-ablated tin and lead atom reactions with H_2O_2 and $H_2 + O_2$ in solid argon and identify the new metal hydroxide molecules M(OH), $M(OH)_2$ and $M(OH)_4$ (M = Sn, Pb).

Experimental and Computational Methods

Laser-ablated Sn and Pb atom reactions with oxygen and with hydrogen in excess argon at 10 K have been described in our previous papers.[9] The Nd:YAG laser fundamental (1064 nm, 10 Hz repetition rate with 10 ns pulse width) was focused onto the rotating high purity metal targets (Johnson Matthey), which gave bright plumes spreading uniformly to the cold CsI window. The tin and lead targets were polished to remove the oxide coating and immediately placed in the vacuum chamber. The laser energy was varied about 10−20 mJ/pulse. Since the tin and lead targets eroded rapidly during the ablation because of metal softness, the targets were adjusted every 5 min to get a fresh surface. FTIR spectra were recorded at 0.5 cm^{-1} resolution on Nicolet 750 with 0.1 cm^{-1} accuracy using an MCTB detector. Matrix samples were annealed at different temperatures, and selected samples were irradiated by a medium-pressure mercury arc lamp (Philips, 175 W) with the globe removed.[14]

Urea hydrogen peroxide (UHP) (Aldrich, 98%) was used as the H_2O_2 source.[13,15] At room-temperature UHP was put into a Chemglass high vacuum valve with Teflon stem and argon gas was passed over the sample to provide H_2O_2. Deuterated urea−D_2O_2 was prepared following previous workers.[16] Samples of H_2, D_2, HD, O_2, $^{18}O_2$, and $^{16,18}O_2$ were diluted in argon as received.

Complementary MP2 calculations were performed using the Gaussian 98 program system,[14] the 6-311++G(3df,3pd) basis set for hydrogen and oxygen atoms, and Los Alamos ECP plus DZ (LANL2DZ) for tin and lead.[17] All geometrical parameters were fully optimized and the harmonic vibrational frequencies were obtained analytically at the optimized structures. Additional B3LYP density functional calculations were done for comparison.

Results

Infrared spectra of products formed in the reactions of laser-ablated lead and tin atoms with H_2O_2 or H_2 and O_2 mixtures in excess argon during condensation at 10 K will be presented in turn. Theoretical calculations were performed to support the identifications of new tin and lead hydroxide molecules. The metal oxides and hydrides produced in these experiments have been assigned in previous studies.[8,9] Common species generated by the laser-ablation process and trapped in solid argon, such as O_3, O_4^-, HO_2, and Ar_nH^+ have been discussed in previous papers.[18−23]

Pb + H_2O_2. Infrared spectra of laser-ablated lead atoms with H_2O_2 in excess argon at 10 K, with annealing and irradiation afterward, (Figure 1) show the following spectral features: (i)

* Corresponding author. E-mail: lsa@virginia.edu.

10.1021/jp053420p CCC: $30.25
Published on Web 09/21/2005

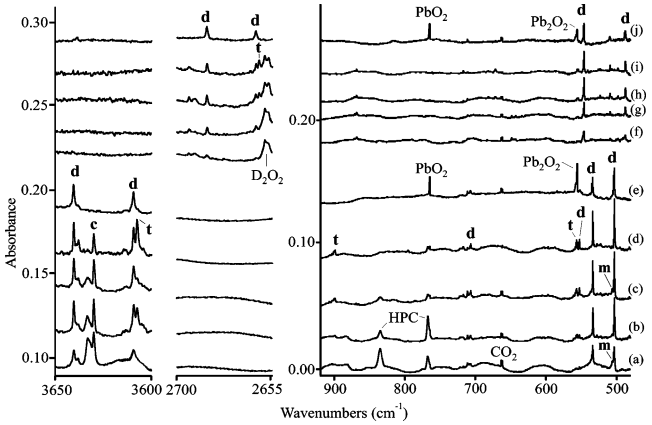

Figure 1. Infrared spectra in selected regions for laser-ablated lead atom reaction products with hydrogen peroxide in excess argon at 10 K: (a) spectrum of Pb and H_2O_2 codeposited for 60 min; (b) spectrum after annealing to 24 K; (c) spectrum after >220 nm irradiation, (d) spectrum after annealing to 34 K, (e) spectrum of Pb + H_2 +O_2 codeposited for 60 min, after ultraviolet irradiation and annealing to 22 K, (f) spectrum of Pb and D_2O_2 codeposited for 60 min, (g) spectrum after annealing to 24 K, (h) spectrum after >220 nm irradiation, (i) spectrum after annealing to 34 K, and (j) spectrum of Pb + D_2 +O_2 codeposited for 60 min, after ultraviolet irradiation and annealing to 22 K. The label C denotes the HOH···O complex (see text) and HPC indicates an aggregate species common to laser-ablation experiments with hydrogen peroxide.

TABLE 1: New Infrared Absorptions (cm^{-1}) Produced on Reactions of Pb + H_2O_2 and Pb + H_2 + O_2 in Excess Argon

H_2O_2 $^{16}O_2$, H_2	$^{16,18}O_2$, H_2	D_2O_2 $^{18}O_2$, H_2	$^{16}O_2$, D_2	identification
3640.2	3640.2, 3629.0	3628.9	2685.4	$Pb(OH)_2$
3609.3	3609.3, 3598.1	3598.0	2661.9	$Pb(OH)_2$
3607.5			2660.4	$Pb(OH)_4$
899.3			671.8	$Pb(OH)_4$
706.8			545.9	$Pb(OH)_2$
556.6			555.4	$Pb(OH)_4$
552.5				$Pb(OH)_2$
533.5	533.7, 530.8, 517.2, 507.0	507.0	509.0	$Pb(OH)_2$
506.1				Pb(OH)
502.7	502.9, 492.5, 480.0, 477.6	477.6	487.3	$Pb(OH)_2$

On deposition absorptions at 502.7 and 533.5 cm^{-1} (stronger) and 552.5 and 706.8 cm^{-1} (weaker) track with two equal intensity bands at 3609.3 and 3640.2 cm^{-1} (group **d**) are observed. With D_2O_2, these bands shift to 487.3, 509.0, 545.9, 596.2, 2685.3, and 2693.8 cm^{-1}, respectively (Table 1). On annealing to 20 and 24 K the intensities of group **d** bands doubled, and they increased 10% on full arc >220 nm irradiation. (ii) Weak group **t** bands at 556.6, 899.3, and 3607.5 cm^{-1} on deposition increased markedly on ultraviolet irradiation. With D_2O_2 the bands shifted to 555.4, 671.8, and 2684.6 cm^{-1}, respectively. (iii) A weak group **m** shoulder absorption observed at 506.1 cm^{-1} beside the 502.7 cm^{-1} band on deposition decreased on annealing but increased on broadband irradiation (note the absence of a shoulder on the 533.5 cm^{-1} band). In addition weak lead oxide absorptions were observed at 711.2 cm^{-1} (PbO), 764.8 cm^{-1} (PbO_2), and 555.6, 466.4 cm^{-1} (Pb_2O_2) in agreement with previous work.[8,9] These bands appeared on deposition and decreased on annealing. Finally, absorptions common to hydrogen peroxide experiments with laser-ablated metals (labeled C) appear at 3730 and 3633 cm^{-1} for the HOH···O complex identified previously.[13,16]

Pb + H_2 + O_2. Complementary experiments were done with Pb/O_2/H_2 in excess argon. On deposition stronger lead oxide bands and weaker lead hydride bands for PbH (1472.3 cm^{-1}) and PbH_2 (1532.7 cm^{-1}) were observed.[9b] In addition broader

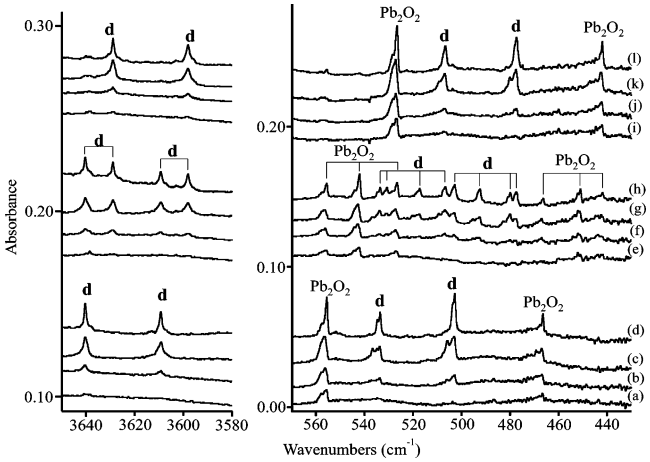

Figure 2. Infrared spectra in the O−H and Pb−O stretching regions for Pb and H_2 + O_2 reaction products in excess argon at 10 K: (a) spectrum of Pb + H_2(6%) + O_2(0.4%) codeposited for 60 min, (b) spectrum after 240−380 nm irradiation, (c) spectrum after >220 nm irradiation, (d) spectrum after annealing to 20 K, (e) spectrum of Pb + H_2(6%) + $^{16,18}O_2$[20% $^{16}O_2$ + 50% $^{16}O^{18}O$ + 30% $^{18}O_2$](0.4%), (f) after 240−380 nm irradiation, (g) spectrum after >220 nm irradiation, (h) spectrum after annealing to 20 K, (i) spectrum of Pb + H_2(6%) + $^{18}O_2$(0.4%) codeposited for 60 min, (j) spectrum after 240−380 nm irradiation, (k) spectrum after >220 nm irradiation, and (l) spectrum after annealing to 20 K.

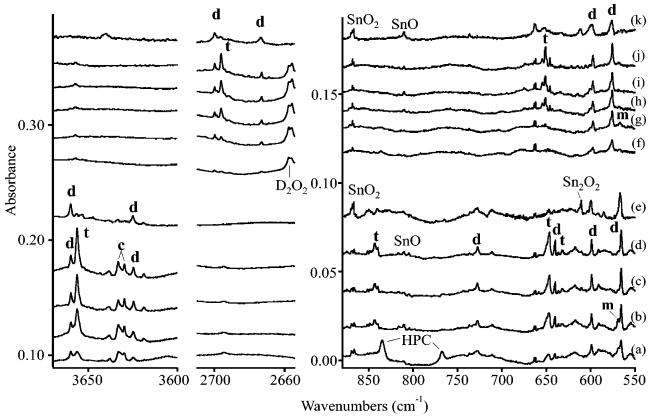

Figure 3. Infrared spectra in selected regions for laser-ablated tin atom reaction products with hydrogen peroxide in excess argon at 10 K: (a) spectrum of Sn and H_2O_2 codeposited for 60 min, (b) spectrum after >220 nm irradiation, (c) spectrum after annealing to 26 K, (d) spectrum after second >220 nm irradiation, (e) spectrum of Sn + H_2 +O_2 codeposited for 60 min, after ultraviolet irradiation and annealing to 22 K, (f) spectrum of Sn and D_2O_2 codeposited for 60 min, (g) spectrum after 240−380 nm irradiation, (h) spectrum after >220 nm irradiation, (i) spectrum after annealing to 24 K, (j) spectrum after annealing to 28 K, and (k) spectrum of Sn + D_2 +O_2 codeposited for 60 min, after ultraviolet irradiation and annealing to 22 K. The label C denotes the HOH···O complex (see text) and HPC indicates an aggregate species common to laser-ablation experiments with hydrogen peroxide.

group **d** product bands appeared very weakly. On >380 nm irradiation, the PbH_2 band disappeared and group **d** product bands increased slightly. Further ultraviolet irradiation increased group **d** bands markedly as well as lead oxide bands. The group **d** bands were observed within 0.3 cm^{-1}of the positions using H_2O_2, but the bands due to group **t** and **m** were not observed in this experiment (shoulders are observed on both broader group **d** bands). One spectrum after ultraviolet irradiation and annealing is compared in Figure 1e. With Pb + D_2 + O_2, the group **d** product bands in Figure 1j show the same shifts as with D_2O_2. In addition, we observed lead deuteride bands for PbD (1055.3 cm^{-1}) and PbD_2 (1099.3 cm^{-1}) and the same lead oxide

TABLE 2: New Infrared Absorptions (cm^{-1}) Produced on Reactions of Sn + H_2O_2 and Sn + H_2 + O_2 in Excess Argon

H_2O_2 $^{16}O_2$, H_2	$^{16,18}O_2$, H_2	$^{18}O_2$, H_2	$^{16}O_2$, HD	D_2O_2 $^{16}O_2$, D_2	$^{18}O_2$, D_2	identification
3659.8	3660.0, 3684.5	3648.5	3660.3, 3625.1	2699.7	2683.3	$Sn(OH)_2$
3656.3				2696.0		$Sn(OH)_4$
3625.1	3625.1, 3613.7	3613.7	2699.6, 2673.1	2673.5	2657.2	$Sn(OH)_2$
843.3				656.9, 646.1		$Sn(OH)_4$
727.4		724.2		646.1		$Sn(OH)_2$
646.5						$Sn(OH)_4$
640.0						$Sn(OH)_2$
631.9						$Sn(OH)_4$
598.8	599.5, 596.7 580.7, 570.2	570.5	601	597.3	571.6	$Sn(OH)_2$
569.5				567.6		Sn(OH)
565.7	566.2, 556.1 541.8, 539.3	539.1	569	575.7	531.2	$Sn(OH)_2$

TABLE 3: Calculated Frequencies for M(OH) and HMO (M = Pb, Sn) at the MP2 Level of Theory and Comparison with Observed of Frequencies

Pb(OH)		Pb(OD)				
calcd[a]	obsd[b]	calcd[a]	obsd[b]	Pb(^{18}OH) calcd[a]	HPbO calcd[a]	assignment
3899.8 (83)		2839.7 (56)		3886.9 (80)	[1608.6 (806)]	O−H [Pb−H] stretching
641.6 (40)		462.9 (5)		639.9 (38)	609.9 (44)	Pb−O−H bending
512.3 (144)	506.1	511.3 (161)		485.5 (131)	489.4 (115)	Pb−O stretching
Sn(OH)		**Sn(OD)**				
calcd[a]	obsd[b]	calcd[a]	obsd[b]	Sn(^{18}OH) calcd	HSnO calcd	assignment
3916.4 (92)		2852.0 (60)		3903.4 (89)	[1765.1 (456)]	O−H [Sn−H] stretching
655.0 (31)		475.3 (29)		653.1 (34)	564.7 (26)	Sn−O−H bending
576.8 (169)	569.5	574.4 (146)	577.8	548.2 (151)	515.9 (66)	Sn−O stretching

[a] Frequencies, cm^{-1} (intensities, km/mol). [b] Argon matrix, cm^{-1}.

bands.[9a,b] A sample of $^{18}O_2$ + H_2 gave ^{18}O shifts as listed in Table 1. With scrambled isotopic O_2 (20% $^{16}O_2$ + 50% $^{16}O^{18}O$ + 30% $^{18}O_2$) the two lower bands for group **d** exhibited quartet distributions while the upper two bands revealed a doublet band.

Sn + H_2O_2. As shown in Figure 3 laser-ablated Sn atom reactions with H_2O_2 in excess argon gave new absorptions at 565.7, 598.8, 640.0, 727.4, 3625.1, and 3656.3 cm^{-1} (group **d**), at 631.9, 646.5, 843.3, and 3618.7 cm^{-1} (group **t**), and at 569.5 cm^{-1} (group **m**). On annealing to 20 K, all product bands increased slightly, and on broadband irradiation, group **d** bands increased by 20% and group **t** bands by 150%, but group **m** changed very little. Further annealing sharpened group **d** and **t** bands but destroyed group **m** bands. Experiments with D_2O_2 gave large red shifts for all upper bands and small shifts for all lower bands, and the results are listed in Table 2. Weak tin oxide bands were observed (SnO, 811.7 cm^{-1}; SnO_2, 867.1 cm^{-1}; Sn_2O_2, 610.7, 521.5 cm^{-1} in solid argon).

Additional Sn + H_2O_2 experiments were done under different conditions. Higher laser energy and laser plume irradiation markedly increased the **t** bands relative to the **d** bands. Next, the H_2O_2 sample tube was surrounded with ice and the H_2O_2 precursor absorption intensities were reduced 10-fold: A comparable Sn experiment resulted in an 8-fold reduction of the strong **t** absorption at 3656.3 cm^{-1} relative to **d** at 3659.8 cm^{-1}. The six **d** absorptions were observed with reduced intensity, but the 646.5 cm^{-1} **t** band was not detected.

Sn + H_2 + O_2. Experiments with Sn and H_2 + O_2 reproduced the new bands as observed with Sn + H_2O_2, but the bands were broadened and shifted slightly. The tin oxide absorptions were stronger with weaker tin hydrides (SnH, 1641.7 cm^{-1}; SnH_2, 1657.0, 1654.8 cm^{-1}).[9,24] These bands appeared on deposition and increased markedly on broadband photolysis. The deuterium counterparts were observed accordingly using Sn + D_2 + O_2 sample. Tin reactions were done with HD + O_2, and the results are shown in Figure 4. Additional experiments with $^{18}O_2$ and $^{16,18}O_2$ (scrambled) gave shifted bands, and the absorptions are listed in Table 2.

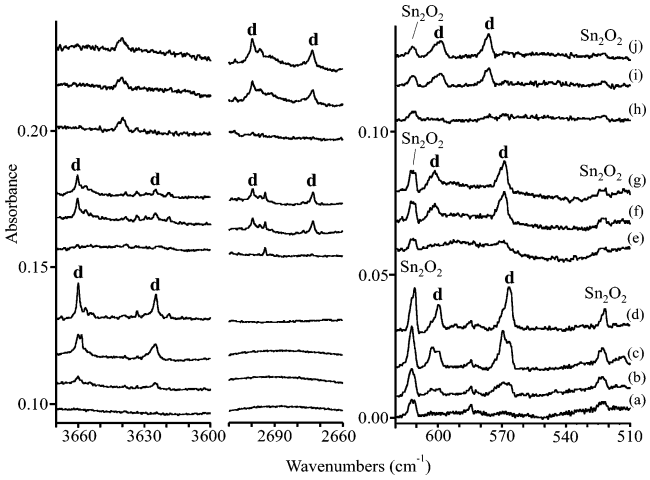

Figure 4. Infrared spectra in the O−H, O−D, and Sn−O stretching regions for Sn and H_2 + O_2 reaction products in excess argon at 10 K: (a) spectrum of Sn + H_2(6%) + O_2(0.4%) codeposited for 60 min, (b) spectrum after 240−380 nm irradiation, (c) spectrum after >220 nm irradiation, (d) spectrum after annealing to 20 K, (e) spectrum of Sn + HD(6%) + O_2(0.4% O_2), (f) spectrum after >220 nm irradiation, (g) spectrum after annealing to 16 K, (h) spectrum of Sn + D_2(6%) + O_2(0.4%) codeposited for 60 min, (i) spectrum after >220 nm irradiation, and (j) spectrum after second >220 nm irradiation.

Calculations. Lead and tin mono-, di-, and tetrahydroxides were calculated at MP2 and B3LYP levels of theory to assist in new product identification. Computations for Pb(OH) gave PbOH and HPbO conformers; however, PbOH is 72 kcal/mol lower in energy than HPbO at the MP2 level. The analogous SnOH molecule is computed to be 55 kcal/mol lower than

TABLE 4: Calculated Frequencies for $Pb(OH)_2$ (C_s), $Pb(OH)_2$ (C_{2v}), and HPbO(OH) at the MP2 Level of Theory and Comparison with Observed Frequencies

$Pb(OH)_2$ (C_s)		$Pb(OD)_2$ (C_s)		$Pb(^{18}OH)_2$ (C_s)				
calcd[a]	obsd[b]	calcd[a]	obsd[b]	calcd[a]	obsd[b]	$Pb(OH)_2$ (C_{2v}) calcd[a]	HPbO(OH) calcd[a]	approximately mode
3905.3 (58)	3640.2	2843.3 (43)	2693.8	3892.5 (56)	3628.9	3900.3 (a_1, 75)	3868.3 (79)	O−H stretching
3861.1 (60)	3609.3	2810.2 (42)	2685.3	3848.5 (57)	3598.0	3899.0 (b_2, 11)	[1933.7 (106)]	O−H stretching [Pb−H]
736.1 (40)	706.8	557.6 (81)	596.2	732.0 (37)		691.6 (a_1, 1)	843.9 (65)	Pb−O−H bending
646.0 (52)	552.5	524.4 (113)	545.9	634.2 (48)		560.9 (b_2, 81)	808.5 (121)	Pb−O−H bending
531.5 (111)	533.5	497.7 (113)	509.0	503.9 (102)	507.0	517.9 (a_1,98)	555.6 (23)	Pb−O stretching
501.7 (144)	502.7	466.5 (7)	487.3	475.7 (131)	477.6	496.1 (b_2, 174)	503.4 (116)	Pb−O stretching
460.7 (74)		340.8 (48)		458.3 (71)		385.8 (b_1, 241)	467.5 (19)	
343.4 (136)		254.1 (76)		341.6 (131)		293.3 (a_2, 0)	360.9 (109)	
166.1 (13)		154.3 (11)		158.6 (11)		176.6 (a_1, 21)	162.7 (55)	

[a] Frequencies, cm^{-1} (intensities, km/mol). [b] Argon matrix, cm^{-1}.

TABLE 5: Calculated Frequencies for $Sn(OH)_2$ (C_s), $Sn(OH)_2$ (C_{2v}), and HSnO(OH) at the MP2 Level of Theory and Comparison with Observed Frequencies

$Sn(OH)_2$ (C_s)		$Sn(OD)_2$ (C_s)		$Sn(^{18}OH)_2$ (C_s)				
calcd[a]	obsd[b]	calcd[a]	obsd[b]	calcd[a]	obsd[b]	$Sn(OH)_2$ (C_{2v}) calcd [a]	HSnO(OH) calcd[a]	approx mode
3902.9 (66)	3660.0	2841.6 (46)	2696.0	3890.1 (63)	3648.5	3894.6 (a_1, 5)	3898.4 (93)	O−H stretching
3857.4 (57)	3625.1	2807.4 (40)	2673.0	3844.8 (55)	3613.7	3894.3 (b_2, 138)	[2013.5 (104)]	O−H stretching [Sn−H]
782.3 (43)	727.4	573.3 (93)	646.1	778.0 (40)	724.2	762.7 (a_1, 80)	839.9 (32)	Sn−O−H bending
697.5 (69)	640.0	567.5 (118)	597.3	694.5 (64)		709.6 (b_2, 58)	823.8 (130)	Sn−O−H bending
573.9 (115)	598.8	535.9 (114)	575.7	545.7 (107)	570.5	569.2 (a_1, 102)	624.2 (112)	Sn−O stretching
541.6 (146)	565.7	504.9 (6)		515.1 (135)	539.1	551.0 (b_2, 167)	601.1 (112)	Sn−O stretching
470.6 (70)		348.3 (45)		468.2 (68)		423.1 (b_1, 172)	461.5 (14)	
359.4 (132)		265.9 (72)		357.5 (130)		355.4 (a_2, 0)	348.5 (140)	
182.0 (15)		169.1 (13)		174.0 (14)		200.3 (a_1, 1)	189.8 (58)	

[a] Frequencies, cm^{-1} (intensities, km/mol). [b] Argon matrix, cm^{-1}.

HSnO. The calculated frequencies are given in Table 3. Our B3LYP calculations gave similar results. A previous combined B3LYP/CCSD investigation found PbOH to be 54 kcal/mol lower energy than HPbO.[6]

For $[Pb(OH)_2]$ three different conformers, $Pb(OH)_2$ (C_s), $Pb(OH)_2$ (C_{2v}), and HPbO(OH) were calculated, and the C_s and C_{2v} structures are very close in energy while HPbO(OH) is 79 kcal/mol higher. Note that the C_s structure is stabilized on the potential energy surface by a weak internal hydrogen bond. At the MP2 level, we use 6-311++(d,p) for H and O and find a H_a-O_b distance of 2.777 Å, which is reduced to 2.714 Å with the large 6-311++G(3df,3pd) basis set. Apparently polarization and diffuse functions for H and O atoms are critical to describe the hydrogen bond. As we will discuss later, the calculated frequencies match experimental values much better using large basis sets. Similar calculations for $Sn(OH)_2$ and at the MP2 level find that $Sn(OH)_2$ lies lowest in energy while $Sn(OH)_2$ (C_{2v}) is 2.8 kcal/mol higher and HSnO(OH) is 40.0 kcal/mol higher in energy. The weak H_a-O_b hydrogen bond is shorter, 2.664 Å, for the tin dihydroxide. The calculated frequencies are listed in Tables 4 and 5.

The B3LYP density functional gave comparable structures for the dihydroxides of Sn and Pb. For $Sn(OH)_2$, the B3LYP functional found 3% shorter Sn−O bond lengths and other parameters almost the same. For $Pb(OH)_2$, the computed structures were almost identical, and the B3LYP frequencies were slightly lower as expected.[26]

Calculations were also done for $Pb(OH)_4$ and $Sn(OH)_4$, and stable S_4 symmetry structures were converged instead of T_d symmetry found for the $Hf(OH)_4$ and $Zr(OH)_4$ molecules.[13d] The structures and parameters are given in Figure 5, and frequencies are listed in Table 6 for the MP2 level calculations. The bent M−O−H bond angles obtained for all lead and tin hydroxides suggest that the molecules exhibit substantial covalent bonding character.[25] The B3LYP functional gave almost identical computed structures for both $M(OH)_4$ molecules.

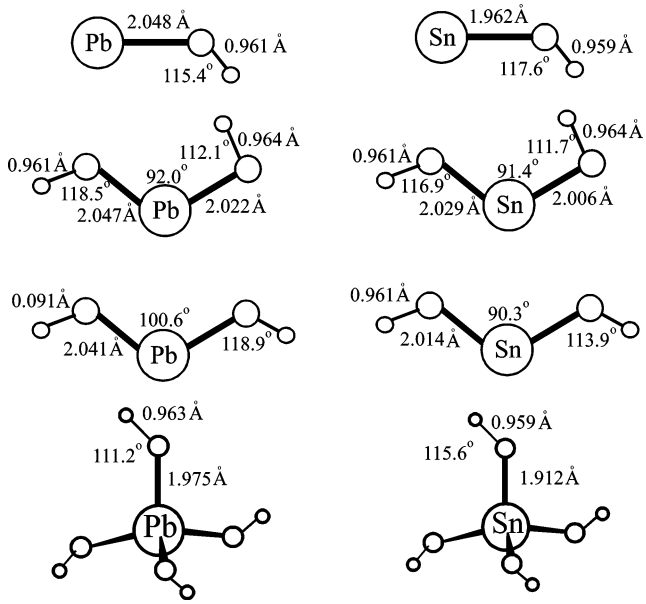

Figure 5. Structures computed for lead and tin hydroxides at the MP2/6-311++G(3df,3pd)/LANL2DZ level of theory. Bond lengths are given in angstroms and bond angles in degrees.

Discussion

The new lead and tin mono-, di-, and tetrahydroxides will be identified through the use of different reagents, photochemical properties, isotopic substitution, and comparison with theoretical frequency calculations.

$Pb(OH)_2$. Two strong new infrared absorptions at 533.5 and 502.7 cm^{-1} in the Pb−O stretching region and two new bands

TABLE 6: Calculated Frequencies for $Pb(OH)_4$ and $Sn(OH)_4$ at the MP2 Level of Theory in S_4 Symmetry and Comparison with Observed Frequencies

$Pb(OH)_4$		$Pb(OD)_4$		$Sn(OH)_4$		$Sn(OD)_4$		
calcd[a]	obsd[b]	calcd[a]	obsd[b]	calcd[a]	obsd[b]	calcd[a]	obsd[b]	approx mode
3881.5 (0)		2826.5 (0)		3928.5 (0)		2861.2 (0)		O−H stretching
3879.5 (44)		2823.8 (28)		3927.2 (56)		2858.8 (37)		O−H stretching
3879.2 (150 × 2)	3607.5	2823.7 (99 × 2)	2684.6	3926.6 (144 × 2)	3656.3	2858.6 (96 × 2)	2696.0	O−H stretching
878.6 (89 × 2)	899.3	653.5 (77 × 2)	671.8	822.8 (115 × 2)	843.3	610.4 (35 × 2)		M−O−H bending
876.8 (60)		652.6 (63)		815.7 (55)		602.7 (6)		M−O−H bending
861.3 (0)		625.7 (0)		802.0 (0)		606.7 (0)		M−O−H bending
565.6 (99 × 2)	556.6	555.9 (75 × 2)	555.4	638.7 (136 × 2)	646.5	636.3 (165 × 2)	654.4	M−O stretching
556.7 (99)		545.8 (65)		626.9 (127)	631.9	624.4 (139)	650.9	M−O stretching
542.8 (0)		536.9 (0)		610.5 (0)		580.8 (0)		M−O stretching
261.0 (176)		210.5 (117)		275.2 (169)		233.8 (119)		
227.0 (48 × 2)		175.9 (51 × 2)		236.6 (66 × 2)		199.3 (57 × 2)		
178.7 (24)		168.7 (6)		215.5 (29)		199.4 (1)		
163.9 (0)		129.6 (0)		173.5 (0)		57.7 (0)		
162.7 (23 × 2)		146.6 (3 × 2)		193.1 (12 × 2)		159.3 (2 × 2)		
129.7 (0)		116.4 (0)		151.4 (0)		118.0 (0)		
92.5 (57)		81.5 (48)		101.6 (104)		86.3 (80)		

[a] Frequencies, cm^{-1} (intensities, km/mol). The a mode has 0 intensity and the b mode has the given intensity, and the e mode has ×2 intensity. [b] Argon matrix, cm^{-1}.

at 3640.2 and 3609.3 cm^{-1} in the O−H stretching region labeled **d** track together in the Pb + H_2O_2 experiments. In the reaction with D_2O_2, the Pb−O bands shift to 509.0 and 487.3 cm^{-1} and the O−H bands to 2685.4 and 2661.9 cm^{-1}, respectively. The red-shift of Pb−O stretching modes with deuterium substitution indicates that these two modes are coupled to the H atom motion. The Pb−O stretching frequencies of PbO and PbO_2 in solid argon at 711.2 and 764.8 cm^{-1} show considerable differences in PbO bonding for the new product molecule. Complementary experiments with Pb + H_2 + O_2 gave slightly broader bands centered at 533.5 and 502.7 cm^{-1} and at 3640.2 and 3609.3 cm^{-1}, which shift to 507.0 and 477.6 cm^{-1} and to 3628.9 and 3598.0 cm^{-1} with Pb + H_2 + $^{18}O_2$. The isotopic frequency ratios for the upper bands (H/D, 1.3556, 1.3559 and 16/18, 1.00311, 1.00314) are characteristic of O−H stretching modes, and the 16/18 ratios for the lower bands (1.0523, 1.0526) describe an antisymmetric O−Pb−O stretching mode (the ratios for PbO_2 (1.0513) and PbO (1.0561) are distinctly different).[9a] The isotopic frequency patterns with $^{16}O_2$ + $^{16,18}O_2$ + $^{18}O_2$ (1:2:1) show quartet distributions for the two lower modes (Figure 2), demonstrating that two inequivalent oxygen atoms are involved. However, for the two upper modes two doublets were observed at 3640.4, 3629.0 cm^{-1} and at 3609.3 and 3598.1 cm^{-1}, which indicate very little or no coupling between two inequivalent O−H groups. Therefore, the $Pb(OH)_2$ molecule with two inequivalent O−H subunits is identified, and the group **d** bands are assigned accordingly. This is distinctively different from group 2, 4, and 12 dihydroxides, which exhibited one strong antisymmetric stretching mode in the O−H and M−O stretching regions for these $M(OH)_2$ molecules with two equivalent O−H subunits.[13]

The identification of $Pb(OH)_2$ is confirmed by MP2 frequency calculations (Table 4). The planar C_s structure at the MP2 level gives two strong Pb−O stretching modes calculated at 531.5 and 501.7 cm^{-1}, which are in excellent agreement with the 533.5 and 502.7 cm^{-1} observed values. The two modes are predicted to red-shift by 33.8 and 35.2 cm^{-1} for $Pb(OD)_2$, which are larger than the experimental shifts of 24.5 and 15.4 cm^{-1}. Obviously the theoretical calculation predicts more H atom coupling than is observed for the two modes. It is interesting to note that the 533.5 cm^{-1} band has a greater deuterium shift than the 502.7 cm^{-1} band, which tells us that the two modes couple with H (and D) atoms differently for this asymmetric structure. The predicted $^{18}O_2$ shifts are slightly more than experimental, but the calculated quartet isotopic patterns for each mode match experiment very well. With MP2 two O−H stretching modes are predicted at 3905.3 and 3861.1 cm^{-1} with almost the same intensities, which are overestimated by 8.2% and 6.1%, respectively, and are in line with expectations.[26] Meanwhile the calculation reveals identical O−H stretching modes for O atoms substituted by $^{18}O_2$ or $^{16,18}O_2$, showing no coupling between the two O−H stretching modes.

The two sharp weaker group **d** bands at 706.8 and 552.5 cm^{-1} are 4 and 14% below the calculated O−H bending frequencies. Clearly, the free O−H bending mode is described better by the MP2 calculation that the O−H group involved in the weak intramolecular hydrogen bond. The 706.8 cm^{-1} band shifts to 545.9 cm^{-1} with D_2O_2 (H/D ratio 1.2947) and gains considerable intensity from mixing with Pb−O stretching modes. The deuterium counterpart for the weaker 552.5 cm^{-1} band is not detected.

Calculations for $Pb(OH)_2$ with the C_s structure using B3LYP give slightly lower Pb−O stretching modes at 523.4 and 494.5 cm^{-1} and O−H stretching modes at 3862.6 and 3825.3 cm^{-1}. However predicted deuterium shifts are only 2−3 cm^{-1} for both Pb−O stretching modes, meaning that the B3LYP calculation does not describe these modes as well as MP2. Our B3LYP calculation found for the optimized structure a H_b-O_a distance 0.043 Å longer than the MP2 value, and as a result the H atom coupling is underestimated.

On the other hand, frequencies calculated for the C_{2v} structure (Table 4) have several shortcomings. The computed O−H stretching mode separation of 1.3 cm^{-1} for two equivalent bonds is far from the observed 30.9 cm^{-1} and C_s computed 44.2 cm^{-1} values, and the 21.8 cm^{-1}computed Pb−O stretching mode separation is in poor agreement with the observed 30.8 cm^{-1} and C_s computed 29.8 cm^{-1} values. Finally, the C_{2v} structure has only one bending mode with observable intensity and the C_s structure has two in good agreement with the observed absorptions.

The insertion reaction of Pb into H_2O_2 is exothermic by 148 kcal/mol (MP2) and 131 kcal/mol (B3LYP), as shown in reaction 1. Spontaneous insertion reaction is observed on annealing of Pb + H_2O_2 suggesting that no activation energy is required. Similar insertion reactions were observed for group 2, 4,and 12 metals.[13] For the reaction of Pb + O_2 + H_2, we

propose that OPbO is formed first on photolysis, and then reacts further with H_2 in the solid matrix cage to give $Pb(OH)_2$. Reaction 2b is 105 kcal/mol exothermic (MP2 level).

$$Pb + H_2O_2 \rightarrow Pb(OH)_2 \quad (\Delta E = -148 \text{ kcal/mol}) \quad (1)$$

$$Pb + O_2 \rightarrow OPbO \quad (\Delta E = -74 \text{ kcal/mol}) \quad (2a)$$

$$OPbO + H_2 \rightarrow Pb(OH)_2 \quad (\Delta E = -105 \text{ kcal/mol}) \quad (2b)$$

$Pb(OH)_4$. Three new infrared absorptions at 556.6, 899.3, and 3607.5 cm^{-1} labeled **t** in $Pb + H_2O_2$ experiments appeared very weakly on deposition and increased upon sample irradiation and annealing, but these bands were not observed with the hydrogen/oxygen reagent. With $Pb + D_2O_2$ these bands shifted to 555.4, 671.8, and 2660.4 cm^{-1}, giving H/D isotopic ratios of 1.0022, 1.3386, and 1.3560, respectively. Apparently the 556.6 cm^{-1} band has a very small deuterium shift, and it can be assigned to the Pb−O stretching mode. The 899.3 and 3607.5 cm^{-1} bands have large deuterium shifts, which are due to Pb−O−H bending and O−H stretching modes, respectively. These group **t** bands are appropriate for $Pb(OH)_4$. Comparison with frequencies calculated by MP2 and B3LYP show very good agreement with experimental values. Absorptions of $Pb(OH)_4$ are predicted by B3LYP calculation to give a stronger degenerate Pb−O stretching mode at 553.1 cm^{-1}, Pb−O−H bending mode at 880.6 cm^{-1}, and O−H stretching mode at 3837.3 cm^{-1}, and counterparts of $Pb(OD)_4$ are found at 543.2 (Pb−O stretching), 655.5 (Pb−O−H bending), and 2793.3 cm^{-1} (O−H stretching). Our MP2 calculation gives slightly higher frequencies (Table 6). Unfortunately in $Pb + H_2 + O_2$ experiments we did not observe these $Pb(OH)_4$ absorptions because of the different reaction mechanism, and no ^{18}O and $^{16,18}O$ isotopic frequencies were observed to confirm the assignment.

Formation of $Pb(OH)_4$ must come from the reaction of $Pb(OH)_2$ and H_2O_2 (reaction 3), which is exothermic by 65 kcal/mol (MP2) and 49 kcal/mol (B3LYP). Notice that reaction 3 is less than half as exothermic as reaction 1. Lead in the tetravalent state is destabilized in part because of the relativistic effect, which increases *s* orbital ionization energy.[10,11,27] As a result the bond strength is reduced for Pb(IV) species.[28,29] The Pb(IV) halides are much less favorable than Pb(II) halides.[10] The yield of $Pb(OH)_4$ increases significantly on photolysis but barely on annealing, implying much less exothermic reaction. Although no absorption of $Pb(OH)_4$ is detected in the $Pb + O_2 + H_2$ experiment, this is significantly different from Zr and Hf, where the straightforward reactions produce major products, $Zr(OH)_4$ and $Hf(OH)_4$ based on very large computed exothermic reaction energies.[13d]

$$Pb(OH)_2 + H_2O_2 \rightarrow Pb(OH)_4 \quad (\Delta E = -65 \text{ kcal/mol}) \quad (3)$$

The relative stability of $Pb(OH)_4$ and $Pb(OH)_2$ is expected to be comparable to that observed for the chlorides and fluorides, which is better than for the recently described case for PbH_4 and PbH_2.[9c] Although the $PbH_2 + H_2 \rightarrow PbH_4$ reaction is slightly endothermic,[30,31] PbH_4 has been formed from PbH_2 in solid hydrogen.[9c] The corresponding reaction 3 is exothermic, which suggests more stability for $Pb(OH)_4$ than for PbH_4.

Pb(OH). A weak absorption at 506.1 cm^{-1} in $Pb + H_2O_2$ experiments can be tentatively assigned to the Pb−O stretching mode of Pb(OH) based on annealing and photochemical behavior. This species is reduced quickly on annealing but is regenerated on ultraviolet irradiation, and is decreased on further annealing like the behavior of an active radical. The weaker O−H stretching fundamental is probably obscured by the nearby mode for $Pb(OH)_2$. Our MP2 calculation for Pb(OH) predicts the Pb−O stretching mode at 512.3 cm^{-1}, which is in good agreement with the 506.1 cm^{-1} band. Our B3LYP calculation gives a very similar result. The insertion product HPbO is not observed here because of its very high energy relative to PbOH. Unfortunately, the Pb(OD) counterpart is not observed due to lower product yield.

Energetic laser-ablated lead atoms react with H_2O_2 to give excited $Pb(OH)_2$ that can either be trapped in the solid matrix or decomposed to Pb(OH) + OH. On photolysis and further annealing the Pb(OH) absorptions decrease, possibly reacting with OH to give $Pb(OH)_2$. Reaction 4 is exothermic but not nearly as much so as reaction 1.

$$Pb + H_2O_2 \rightarrow [Pb(OH)_2]^* \rightarrow Pb(OH) + OH \quad (\Delta E = -43 \text{ kcal/mol}) \quad (4)$$

$Sn(OH)_2$. The group **d** bands at 565.7, 598.8, 640.0, 727.4, 3625.1, and 3660.0 cm^{-1} track together in experiments with $Sn + H_2O_2$ upon annealing, irradiation, and changes in hydrogen peroxide concentration, and they can be assigned and to $Sn(OH)_2$. The same absorptions were found in $Sn + H_2 + O_2$ reactions but with slightly lower intensities. The 565.7 and 598.8 cm^{-1} bands shift to 539.1 and 570.5 cm^{-1} with $^{18}O_2$ substitution, suggesting two Sn−O stretching modes, while the 640.0 and 727.4 cm^{-1} bands show very small shifts, which are appropriate for the Sn−O−H bending modes. The 3660.0 and 3625.1 cm^{-1} bands exhibited 11.5 and 11.4 cm^{-1} red-shifts in the $Sn + H_2 + {}^{18}O_2$ experiment, which are typical for O−H stretching modes in a metal hydroxide. The oxygen isotopic quartet pattern for both 565.7 and 598.8 cm^{-1} bands and doublets for the 3660.0 and 3625.1 cm^{-1} bands were observed with $^{16}O_2 + {}^{16}O^{18}O + {}^{18}O_2 + H_2$, showing two inequivalent oxygen atoms, which are very similar that found for $Pb(OH)_2$. With D_2O_2 the 598.8 cm^{-1} band shifts red only 1.5 cm^{-1} to 597.3 cm^{-1}, while the 565.7 cm^{-1} band shifts blue by 10.0 cm^{-1}, indicating different couplings of the O−D bending vibrations with these modes. This is not the case for $Pb(OH)_2$, for which both Pb−O modes shift red with deuterium substitution. The O−D stretching modes appeared at 2699.7 and 2673.5 cm^{-1}, giving 1.3556 and 1.3559 H/D ratios, which again are typical for metal dihydroxides.[13] The O−D stretching modes red shifted 16.4 and 16.3 cm^{-1} with $Sn + D_2 + {}^{18}O_2$, which is in line with previous observations.[13] The Sn−^{18}OD stretching modes were observed at 571.6 and 531.2 cm^{-1}. The upper band exhibits a reasonable ^{18}O shift, but the lower band appears to have a considerably different amount of mixing with the Sn−O−D bending mode for the blue shift described above.

The vibrational assignment of $Sn(OH)_2$ is supported by theoretical calculations. Our MP2 calculation shows that two structures, namely C_s and C_{2v}, are very close in energy but very different in frequencies (Table 5). The calculated frequencies of the C_s structure predict the experimental frequencies satisfactorily, but the C_{2v} frequencies suffer from the mode separation deficiencies described above for lead dihydroxide. These are Sn−O stretching modes at 573.9 and 541.6 cm^{-1}, O−H stretching modes at 3902.9 and 3857.4 cm^{-1}, which must be scaled down by 6.2 and 6.0%, respectively, and Sn−O−H bending modes at 782.3 and 697.5 cm^{-1}. It is not surprising that the two predicted quartets for two Sn−O stretching modes and two doublets for O−H stretching modes with ^{16}O and ^{18}O substitution match experimental bands very well. The predicted O−D stretching frequencies at 2841.6 and 2807.4 cm^{-1} are in reasonable agreement (scale down by 5.0 and 4.7%), but the Sn−O stretching modes are predicted to shift down 6.4 and

5.7 cm^{-1}. Apparently the O−H coupling effect for these modes is underestimated. The upper O−H(D) stretching mode is due to the free O−H(D) bond and the lower mode to O−H(D) in the intramolecular hydrogen bond.

The $Sn(OH)_2$ molecule is formed spontaneously from combination of Sn and H_2O_2 (reaction 5), which is exothermic by 154 kcal/mol (MP2) and 145 kcal/mol (B3LYP) and is slightly more exothermic than that found in the lead reaction. Formation of $Sn(OH)_2$ is also through reaction of Sn with H_2 and O_2 (reaction 6), and ultraviolet irradiation promoted this reaction significantly.

$$Sn + H_2O_2 \rightarrow Sn(OH)_2 \quad (\Delta E = -154 \text{ kcal/mol}) \quad (5)$$

$$Sn + O_2 \rightarrow OSnO \quad (\Delta E = -106 \text{ kcal/mol}) \quad (6a)$$

$$OSnO + H_2 \rightarrow Sn(OH)_2 \quad (\Delta E = -79 \text{ kcal/mol}) \quad (6b)$$

[We note that the difference in the energies of reactions 1 and 2 compared to reactions 5 and 6, namely −31 kcal/mol, is in fact the energy of formation of hydrogen peroxide computed at the MP2 level, −31 kcal/mol.]

The Sn, HD, O_2 reaction was done to examine the distribution of isomers involving H or D in the intramolecular hydrogen bonding position, and the spectra are compared in Figure 4 with those from similar H_2 and D_2 experiments. This is analogous to HD and F_2 reactions, which formed primarily the H−F···D−F dimer.[32] Our calculations show no coupling between the O−H(D) bonds so the frequencies are the same for both Sn(OH)(OD) isomers as in the $Sn(OH)_2$ and $Sn(OD)_2$ molecules. Note for the HD + O_2 spectrum that the 3660 and 2673 cm^{-1} bands are 60 ± 10% stronger relative to the 3625 and 2700 cm^{-1} counterparts for $Sn(OH)_2$ and $Sn(OD)_2$. This means that the (HO)Sn(OD) isomer [D···O] is favored over the (DO)Sn(OH) isomer [H···O]. Computed zero point vibrational energies find the former 44 cal/mol more stable. Recall that these molecules are formed in reaction 6b with approximately 79 kcal/mol of excess internal energy.

$Sn(OH)_4$. The group **t** bands at 631.9, 646.5, 843.3, and 3656.3 cm^{-1} are assigned to $Sn(OH)_4$ in the Sn + H_2O_2 experiment. Apparently the 631.9 and 646.5 cm^{-1} bands are due to Sn−O stretching modes and the 3656.3 cm^{-1} band is due to the O−H stretching mode based on similar bond properties with $Sn(OH)_2$. The deuterium counterparts were found at 650.9, 654.4, and 2696.0 cm^{-1} with Sn + D_2O_2. Here both Sn−O modes show blue shifts suggesting strong O−D coupling, since the 843.3 cm^{-1} Sn−O−H bending mode shifts into this region on deuterium substitution as found for the same mode in $Sn(OD)_2$. The $Sn(OH)_4$ molecule is calculated to have S_4 symmetry at MP2 level, and the Sn−O stretching mode splits into an active b component at 626.9 cm^{-1} and a degenerate e mode at 638.7 cm^{-1}, which underestimate the observed values by 5.0 and 7.8 cm^{-1}. The Sn−O stretching modes in $Sn(OD)_4$ are predicted at 624.4 and 636.3 cm^{-1}, respectively, which unfortunately deviate from experimental values. Again the density functional theoretical calculation does not describe the O−H coupling correctly. The predicted b and e O−H stretching modes are too close to resolve. The stronger e mode for $Sn(OH)_4$ at 3926.6 cm^{-1} and O−D stretching mode for $Sn(OD)_4$ at 2858.6 cm^{-1} must scale 6.9 and 5.7% to fit the observed 3656.3 and 2696.0 cm^{-1} bands. Our B3LYP calculation gave very similar results.

The stable $Sn(OH)_4$ molecule is formed by further reaction of $Sn(OH)_2$ with H_2O_2 (reaction 7). This reaction is exothermic by 123 kcal/mol, which is almost twice as high as calculated for the reaction to form $Pb(OH)_4$. Notice that the yield of $Sn(OH)_4$ is slightly higher and weak bands due to $Sn(OH)_4$ were observed in Sn + H_2 + O_2 experiments, indicating $Sb(OH)_4$ is more stable than $Pb(OH)_4$. In fact only $PbCl_4$ is observed experimentally while several SnX_4 (X = Cl, Br, I) molecules have been identified. Tetrahydroxide molecules have also been observed for group 4 metals in even more exothermic reactions with hydrogen peroxide in excess argon.[13d]

$$Sn(OH)_2 + H_2O_2 \rightarrow Sn(OH)_4 \quad (\Delta E = -123 \text{ kcal/mol}) \quad (7)$$

Sn(OH). A weak band at 569.5 cm^{-1} (Sn−O stretching) in Sn + H_2O_2 experiments is tentatively assigned to Sn(OH). With D_2O_2 the band shifts to 567.6 cm^{-1}. These bands appear on sample irradiation along with $Sn(OH)_2$ and $Sn(OD)_2$ and then decrease on further annealing as expected for a reactive species. Our MP2 calculation predicts this Sn−O stretching mode at 576.8 cm^{-1} with a 2.4 cm^{-1} shift for Sn(OD) (Table 3), which are in good agreement. The weaker O−H stretching mode is probably masked by the nearby mode for $Sn(OH)_2$. The formation of Sn(OH) is through reaction 8, and the product is then trapped in the low-temperature matrix.

$$Sn + H_2O_2 \rightarrow [Sn(OH)_2]^* \rightarrow Sn(OH) + OH \quad (\Delta E = -51 \text{ kcal/mol}) \quad (8)$$

Bonding in Group 14 Metal Hydroxides. The C_s symmetry structures calculated and observed for $Pb(OH)_2$ and $Sn(OH)_2$ are unique: (i) the O−M−O bond is close to a right angle, which is very different from group 2 and transition metal hydroxides, (ii) a weak intramolecular hydrogen bond is formed that is not found in other metal hydroxides, and (iii) $Pb(OH)_4$ and $Sn(OH)_4$ are minor reaction products although Pb(IV) and Sn(IV) halides have been observed experimentally.[10] First, MH_2 and MX_2 (M = Pb, Sn, X = halogen) triatomic molecules favor bent structure with near 90° bond angles, which has been explained by pure p orbital bonding because of high s orbital ionization energy.[10,11] However OPbO and OSnO molecules are linear based on matrix infrared spectra and theoretical calculations, which suggests that both *s* and p orbitals participate in this bonding interaction. Recall that group 2 metal hydroxides and oxides have very similar O−M−O bond angles since only two *s* electrons are involved in the bonding.[13] Second, the Pb−O and Sn−O bonds in $Pb(OH)_2$ and $Sn(OH)_2$ have substantial covalent character. The O−H stretching frequencies are very near this mode in the most covalent metal hydroxides such as $Cd(OH)_2$ and $Hg(OH)_2$, (3659.3 and 3629.4 cm^{-1}), but somewhat lower than O−H stretching frequencies in group 2 and group 4 metal hydroxides.[13] Third, the smaller O−Pb−O bond angle provides a shorter distance between O_b and H_a, which attract each other giving extra stabilization energy from a weak intramolecular hydrogen bond. Only the C_s geometry is observed although the calculated energies of the C_s and C_{2v} structures are very close. Finally, the intramolecular hydrogen bond computed here for $Sn(OH)_2$ and $Pb(OH)_2$ is weaker and substantially longer (2.7 Å) than that computed for the strong phenol−ammonia hydrogen bonded complexes (1.9 Å).[33]

The formation of tetrahydroxides of lead and tin is analogous to their tetrahalides. Theoretical calculations show that $Sn(OH)_4$ is more stable than $Pb(OH)_4$, which can be confirmed from experiments in that the yield of $Sn(OH)_4$ is more than that of $Pb(OH)_4$. Obviously relativistic effects play an important role here and cause the lead tetravalent state to be less favorable.[10,11]

The $Sn(OH)_4$ and $Pb(OH)_4$ molecules with S_4 structures and bent M−O−H bonds are clearly more covalent[25] than the Zr-

$(OH)_4$ and $Hf(OH)_4$ molecules with T_d structures.[13d] The O−H stretching frequencies have the same relationship described for the dihydroxides, namely the more covalent Sn and Pb tetrahydroxides have lower (3656.3 and 3607.5 cm^{-1}) O−H modes than the more ionic Zr and Hf tetrahydroxides (3782.6 and 3796.4 cm^{-1}).

Conclusions

Laser-ablated lead and tin atoms react with H_2O_2 to form the hydroxides M(OH), $M(OH)_2$, and $M(OH)_4$ (M = Pb, Sn), which were observed in infrared spectra after sample condensation in solid argon. The major $M(OH)_2$ product was also produced from H_2 and O_2 mixtures, which allowed $^{18}O_2$ substitution. The band assignments were confirmed by appropriate D_2O_2, D_2, $^{16}O^{18}O$, and $^{18}O_2$ isotopic shifts. Complementary MP2 and B3LYP calculations provided molecular structures and vibrational frequencies to aid in assignment of the infrared spectra. The minimum energy structure found for $M(OH)_2$ has C_s symmetry and a weak intramolecular hydrogen bond. In experiments with Sn, HD, and O_2, the internal D bond is favored over the internal H bond for Sn(OH)(OD). Calculations for the $Pb(OH)_4$ and $Sn(OH)_4$ molecules find S_4 symmetry and substantial covalent character, and relativistic effects limit the yield of the less stable lead tetrahydroxide molecule.

Acknowledgment. We appreciate financial support from NSF Grant CHE 03-53487.

References and Notes

(1) Sterckeman, T.; Douay, F.; Proix, N.; Fourrier, H. *Environ. Pollut.* **2000**, *107*, 377.

(2) (a) Abbott, M. B.; Wolfe, A. D. *Science* **2003**, *301*, 1893. (b) Shotyk, W.; Weiss, D.; Appleby, P. G.; Cheburkin, A. K. Frei, R.; Gloor, M.; Kramers, J. D.; Reese, S.; Van Der Knaap, W. O. *Science* **1998**, *281*, 1635.

(3) Carignan, J.; Simonetti, A. Gariepy. C.*Atmos. Environ.* **2002**, *36*, 3759.

(4) Jain, N. B.; Laden, F. Guller, U.; Shankar, A.; Kazani, S.; Garshike, E. *Am. J. Epidemiology* **2005**, *161*, 968.

(5) Endres, J.; Montgomery, J.; Welch, P. *J. Environ. Health* **2002**, *64*, 20.

(6) Benjelloun, A. T.; Daoudi, A.; Chermette, H. *J. Chem. Phys.* **2004**, *121*, 7207.

(7) Ziebarth, K.; Beridhor, R.; Shestakov, O.; Fink, E. H. *Chem. Phys. Lett.* **1992**, *190*, 271.

(8) (a) Ogden, J. S.; Ricks, M. J. *J. Chem. Phys.* **1972**, *56*, 1658 (PbO). (b) Bos, A.; Ogden, J. S. *J. Phys. Chem.* **1973**, *77*, 1513, (Sn + O_2).

(9) (a) Chertihin, G. V.; Andrews, L. *J. Chem. Phys.* **1996**, *105*, 2561, (Pb + O_2). (b) Wang, X.; Andrews, L.; Chertihin, G. V.; Souter, P. F. *J. Phys. Chem. A* **2002**, *106*, 7696, (Pb, Sn + H_2). (c) Wang, X.; Andrews, L. *J. Am. Chem. Soc.* **2003**, *125*, 6581, (Pb + H_2).

(10) Haigittai, M. *Chem. Rev.* **2000**, *100*, 2233 and references therein.

(11) Pyykko, P. *Chem. Rev.* **1988**, *88*, 563.

(12) (a) Cotton, F. A.; Wilkinson, G.; Murillo, C. A.: Bochmann, M. *Advanced Inorganic Chemistry*, 6th ed.; Wiley: New York, 1999. (b) *CRC Handbook*, 66th ed.; CRC Press: Boca Raton, FL, 1985.

(13) (a) Wang, X.; Andrews, L. *J. Phys. Chem. A* **2005**, *109*, 2782 (group 2 metal hydroxides). (b) Wang, X.; Andrews, L. *J. Phys. Chem. A* **2005**, *109*, 3849 (Zn, Cd hydroxides). (c) Wang, X.; Andrews, L. *Inorg. Chem.* **2005**, *44*, 108 ($Hg(OH)_2$). (d) Wang, X.; Andrews, L. *Inorg. Chem.* **2005**, *44*, in press (hafnium metal hydroxides). Wang, X.; Andrews, L. *J. Phys. Chem. A* **2005**, *109*, in press (group 4 metal hydroxides).

(14) Andrews, L. *Chem. Soc. Rev.* **2004**, *33*, 123 and references therein.

(15) Pettersson, M.; Tuominen, S.; Rasanen, M. *J. Phys. Chem. A* **1997**, *101*, 1166.

(16) Pehkonen, S.; Pettersson, M.; Lundell, J.; Khriachtchev, L.; Rasanen, M. J. *Phys. Chem. A* **1998**, *102*, 7643 and references therein.

(17) Frisch, M. J.; Trucks, G. W.; Schlegel, H. B.; Scuseria, G. E.; Robb, M. A.; Cheeseman, J. R.; Zakrzewski, V. G.; Montgomery, J. A., Jr.; Stratmann, R. E.; Burant, J. C.; Dapprich, S.; Millam, J. M.; Daniels, A. D.; Kudin, K. N.; Strain, M. C.; Farkas, O.; Tomasi, J.; Barone, V.; Cossi, M.; Cammi, R.; Mennucci, B.; Pomelli, C.; Adamo, C.; Clifford, S.; Ochterski, J.; Petersson, G. A.; Ayala, P. Y.; Cui, Q.; Morokuma, K.; Malick, D. K.; Rabuck, A. D.; Raghavachari, K.; Foresman, J. B.; Cioslowski, J.; Ortiz, J. V.; Stefanov, B. B.; Liu, G.; Liashenko, A.; Piskorz, P.; Komaromi, I.; Gomperts, R.; Martin, R. L.; Fox, D. J.; Keith, T.; Al-Laham, M. A.; Peng, C. Y.; Nanayakkara, A.; Gonzalez, C.; Challacombe, M.; Gill, P. M. W.; Johnson, B.; Chen, W.; Wong, M. W.; Andres, J. L.; Gonzalez, C.; Head-Gordon, M.; Replogle, E. S.; Pople, J. A. *Gaussian 98*, Revision A.6.

(18) Wang, X.; Andrews, L. *J. Phys. Chem.* A **2001**, *105*, 5812.

(19) Zhou, M.; Hacalogu, J.; Andrews, L. *J. Chem. Phys.* **1999**, *110*, 9450.

(20) Milligan, D. E.; Jacox, M. E. *J. Mol. Spectrosc.* **1973**, *46*, 460.

(21) Jacox, M. E.; Thompson, W. E. *J. Chem. Phys.* **1994**, *100*, 750.

(22) Milligan, D. E.; Jacox, M. E. *J. Chem. Phys.* 1**963**, *38*, 2627.

(23) Smith, D. W.; Andrews, L.*J. Chem. Phys.* 1**974**, *60*, 2627.

(24) See ref 8(a) for Kr matrix observations. In solid argon, $Sn^{16}O$ peaked at 810.2 and $Sn^{18}O$ at 769.9 cm^{-1}. The SnO_2 bands gave resolved ^{116}Sn, ^{118}Sn, and ^{120}Sn isotopic triplets at 870.2, 868.5, and 867.1 cm^{-1} for $Sn^{16}O_2$, at 854.2, 852.7, and 851.2 cm^{-1} for $Sn^{16}O^{18}O$, and at 831.7, 830.1, and 828.5 cm^{-1} for $Sn^{18}O_2$.

(25) Ikeda, S.; Nakajiama, T.; Hirao, K. *Mol. Phys.* **2003**, *101*, 105.

(26) Scott, A. P.; Radom, L. *J. Phys. Chem.* **1996**, *100*, 16502.

(27) Desclaux, J. P.; Pyykko, P. *Chem. Phys. Lett.* **1974**, *29*, 534.

(28) Kaupp, M.; Schleyer, P. v. R. *J. Am. Chem. Soc.* **1993**, *115*, 1061.

(29) Schwerdtfeger, P.; Heath, G. A.; Dolg, M.; Bennett, M. A. *J. Am. Chem. Soc.* **1992**, 114, 7518.

(30) Dyall, K. G.; Taylor, P. R.; Faegri, K.; Partridge. H. *J. Chem. Phys.* **1991**, *95*, 2583.

(31) Dyall, K. G. *J. Chem. Phys.* **1992**, *96*, 1210.

(32) Hunt, R. D.; Andrews, L. *J. Chem. Phys.* **1985**, *82*, 4442.

(33) See for example: (a) Iwasaki, A.; Fujii, A.; Watanabe, T.; Ebata, T.; Mikami, N. *J. Phys. Chem.* **1996**, *100*, 16053. (b) Abkowicz-Bienko, A.; Latajka, Z. *J. Phys. Chem. A* **2000**, *104*, 1004.